I. DETAILS OF SMT DATA ANALYSIS

A. Separation of paired and unpaired *homie* insulator states in [1]

E-P constructs of Chen et al. [1] include two *homie* insulators that can be paired to form a loop, except one control without the insulators. In principle, E-P distance is generally shorter when homie insulators are paired. However, only one peak appears in the original E-P distance distribution, such as in the construct without a promoter [Fig. 1 (a)]. A two-state model describes insulator paring [1]. The states may be indistinguishable due to high randomness in E-P movement and the lower probability of the paired state. Based on state continuity, we smoothed the E-P distance timing profile using a sliding time window (typically, 15 min). The smoothed distribution shows two well-separated peaks [Fig. 1 (b)]. The paired state mainly contribute to the smaller left peak, while the unpaired state contributes to the bigger right peak. The construct without homie insulators shows no two peaks, even after smoothing (Fig. 1). Based on the smoothed E-P distance distribution, we set thresholds at 0.4 μm and 0.7 μm to distinguish paired and unpaired states. The system is paired when the average distance is below the smaller threshold and unpaired when above the greater threshold. The smaller threshold is nearer to the paired peak, while the greater threshold is closer to the unpaired peak, as state mixing is likely in the intermediate range. Further analysis of the original E-P distance timing profile was conducted for both paired and unpaired states. In the unpaired state, the contour length is the linear distance between the enhancer and promoter along the non-intersecting E-P DNA region. In the paired state, the effective contour length is their shortest distance along the genome cross structure formed by homie insulator pairing.

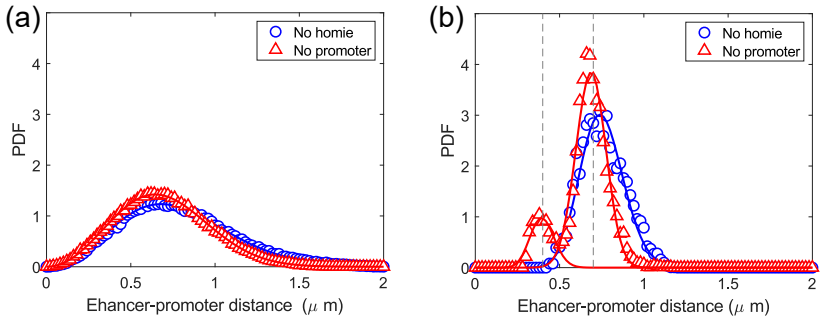

FIG. 1. The paired and unpaired states of constructs with homie insulators [1] were separated by smoothing the E-P distance timing profile. The E-P distance (r) distribution was fitted using $Ar^g \exp(-\alpha r^\delta)$. The green (blue) line shows the construct without the promoter (homie insulators). (a) The E-P distance distribution has one peak for the construct without homie insulators or the promoter. Parameters: $A = 8.36$, $g = 2.05$, $\alpha = 2.45$, $\delta = 2.36$. (b) The smoothed E-P distance distribution has two peaks without the promoter but one without homie insulators. A 15 min sliding window smoothed the E-P distance timing profile. Fitting for no homie used $r > 0.5$ μm, while no promoter fitting used r >0.5 μm and r <0.5 μm separately. Dashed gray lines mark 0.4 and 0.7 μm thresholds. Parameters: $A = 2.86 \times 10^7$, $g = 18.7$, $\alpha = 17.92$, $\delta = 1.79$ (no homie); $A = 4.9 \times 10^5$, $g = 17.48$, $\alpha = 18.39$, $\delta = 3.37$ (no promoter, $r > 0.5\mu m$); $A = 1.67 \times 10^8$, $g = 13.63$, $\alpha = 48.09$, $\delta = 2.19$ (no promoter, $r < 0.5\mu m$).

B. Parameters for determining power-law exponent ν with experimental data

Bead parameters: $R_{linker} = L_{linker} = 3$ nm, $L_{nc} = 50$ nm, $R_{nc} = 10$ nm (*Drosophila*); $R_{linker} = L_{linker} = 0$ nm, $L_{nc} = 50$ nm, $R_{nc} = 6$ nm (mouse).

We used four E-P SMT data groups for *Drosophila* embryos [1] based on insulator paring and gene expression: (I) non-expression (paired), (II) expression (paired), (III) non-expression (unpaired), and (IV) expression (unpaired). The E-P effective contour length (L_{EP}) for unpaired and paired insulators is 52 μm and 7.48 μm, respectively. Average E-P distances (R_{EP}) for groups (I)-(IV) are 0.4, 0.35, 0.79, and 0.68 μm, respectively. Derived ν are 0.6918, 0.6638, 0.6, and 0.58, respectively.

We used four E-P SMT data groups from [1], based on promoter or homie insulator knocked out, insulator paring, and gene expression: (I) -promoter(paired), (II) -promoter(unpaired), (III) non-expression(-homie), and (IV) expression(-homie). L_{EP}= 52 (unpaired) or 7.48 μm (paired). R_{EP} for datasets (I)-(IV) are 0.37, 0.76, 0.78, and 0.75 μm, respectively. Derived ν are 0.68, 0.59, 0.59, and 0.59, respectively.

We used E-P SMT data from three mESC constructs [2]: (I) Sox2-SCR ESC, (II) Sox2-SCRdel ESC, and (III)

Sox2-del-SCR ESC. Effective L_{EP} = 42.5 (I), 39.44 (II), or 4.42 μm (III). R_{EP} for datasets (I)-(III) = 0.34, 0.34, or 0.25 μm. Derived ν = 0.6, 0.6, or 0.83.

We used E-P SMT data from five *Drosophila* embryonic constructs (similar to in [1]) with varying L_{EP} [5]. In the insulator-unpaired state, L_{EP} = 58, 82, 88, 149, or 190 kb, with R_{EP} of 0.52, 0.68, 0.71, 0.74, or 0.82μm, and ν of 0.62, 0.63, 0.63, 0.59, or 0.58. In the paired state, effective $L_{EP} \approx 6.6\mu m$, with R_{EP} of 0.37, 0.43, 0.41, 0.42, 0.42 (non-expression) or 0.38, 0.39, 0.45, 0.38, 0.36 (expression), and ν of 0.69, 0.72, 0.71, 0.72, 0.72 (non-expression) or 0.70, 0.71, 0.73, 0.70, 0.69 (expression).

We used TetO-LacO SMT data from two mESC constructs [6]: (I) +CTCF-RAD21, (II)-CTCF-RAD21. The TetO-LacO contour length is 53 μm. The average TetO-LacO distances for (I) and (II) are 0.37 and 0.39 μm, with ν of 0.59 and 0.6, respectively.

C. Correlation between E-P distance and transcription level

The scatter plot [Fig.2 (a)] shows no significant correlation between E-P distance and transcription level. Considering the possible delay in transcription signal relative to E-P communication, we recalculated the correlation with a fixed delay but still found no significant correlation. This may be due to the delay variability reflected in our dynamic "kissing" model. We defined burst periods as intervals when transcription level exceeds a preset threshold. In the species with insulator, the E-P distance distribution during bursts differs from non-burst periods.Aligning timing profiles during paired periods to burst onset shows a sharp increase in expression after bursting begins, while E-P distance tends to decrease beforehand. These findings suggest a weak correlation between E-P distance and transcription level.

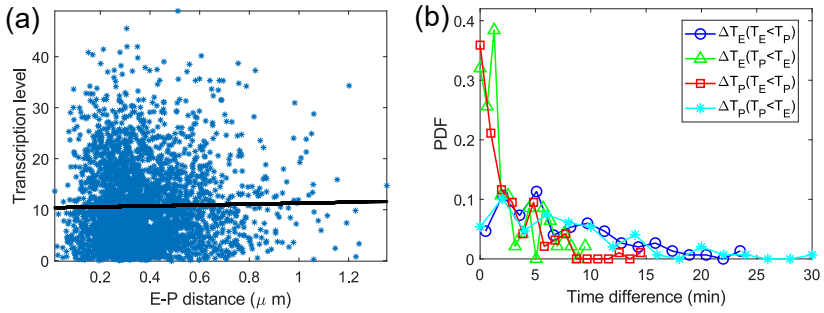

FIG. 2. (a) Scatter plot of E-P distance versus transcription level. Black line represents the linear fit. Pearson r = 0.02; p= 0.27. (b) Probability distribution of the time difference between T_E (or T_P) and T_{EP}. SMT data of [1] were used.

D. Timing of promoter licensed/enhanced

As assumed, the promoter is licensed by epigenetic signals and independently enhanced by the enhancer. A unlicensed promoter cannot initiate transcription, while a licensed promoter transcribes at a low level without enhancement and at a high level with enhancement. We determined promoter licensing (T_P) and enhancement (T_E) times using E-P distance and transcription data. T_P starts at each expression period's onset, while T_E occurs when E-P distance falls below a threshold—typically the average of E-P distance minus its standard deviation. We used the time difference $T_P - T_E$. Full promoter activation (T_{EP}) occurs when the transcription exceeds a threshold (typically 5). Ideally, T_{EP} should equal $\max(T_P, T_E)$ per burst. To verify this, we computed probability distributions of $\Delta T_E = T_{EP} - T_E$ and $\Delta T_P = T_{EP} - T_P$. As expected, when $T_P > T_E$, ΔT_P was tightly clustered but ΔT_E varied widely; when $T_P < T_E$, ΔT_E was tight but ΔT_P scattered [Fig. 2 b].

II. PARAMETERS USED IN THE SIMULATION OF TRANSCRIPTIONAL BURSTING

For the dynamic kissing model, we applied parameters from the *Drosophila* E-P system in the insulator-paired state [1], with a 397-bead polymer chain. Loss rates of the promoter's license and activation signals ($\lambda_{off,1}$ and $\lambda_{off,2}$) were fixed by fitting the time gap between promoter licensing and enhancer activation using the function: $0.5[\lambda_{off,1}\exp(-\lambda_{off,1}t)\theta(t) + \lambda_{off,2}\exp(\lambda_{off,2}t)\theta(-t)]$, where $\theta(t)$ is a unit step function). This yielded $\lambda_{off,1}$ =

$0.11\,\mathrm{min}^{-1}$, and $\lambda_{off,2} = 0.14\,\mathrm{min}^{-1}$. The step interval (0.1 min) and the promoter licensing rate ($\lambda_{on} = 0.3\,\mathrm{min}^{-1}$) were selected by comparing experimental and theoretical results. Given the independence of promoter licensing and enhancer activation, burst duration follows $\lambda \exp(-\lambda t)$, where $\lambda = \lambda_{off,1} + \lambda_{off,2}$, accurately capturing the experimental distribution [Fig. 6(b)]. The E-P communication distance threshold $D_{EP}^{commun} = \langle r \rangle$-$\sigma(r)$ (Fig. 3). Varying the step interval, licensing rate, or D_{EP}^{commun} has no significant effect.

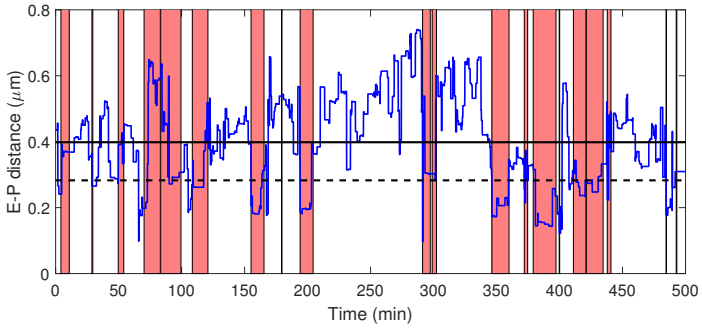

FIG. 3. An arbitrarily selected E-P distance profile from dynamic simulations. The thick black line shows the average distance, while the dashed black line marks the threshold for E-P communication (average -− standard deviation). Red squares indicate transcriptional burst periods.

To simulate transcriptional bursts for various E-P contour lengths, we used a fixed D_{EP}^{commun}. Gene expression and contact probability at different L_{EP} from [3] and [4] were used In the *E.coli* E-P system from [3], the NtrC enhancer was 300-6000 bp from the *glnAp2* promoter driving *lacZ* transcription. Bacteria nucleosome-like particles are ∼13 nm in diameter, containing 220-290 bp of DNA [7]. Parameters for [3]: $D_{EP}^{commun} = 0.07\ \mu m$, $d_{bead} = 13$ nm and $L_{bead} = 53$ nm. The results remained consistent even when each bead contained 220+ bp of DNA [Fig. 4 (a)].

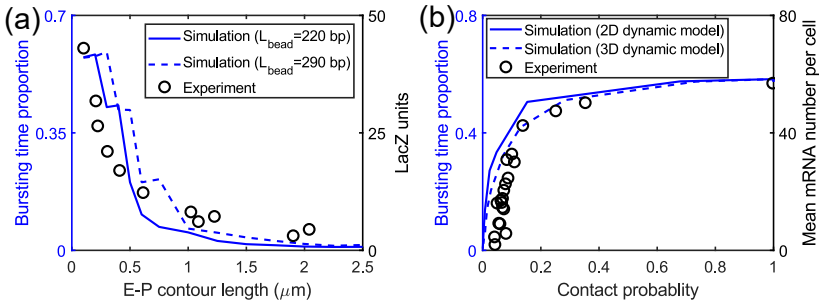

FIG. 4. The E-P dynamic kissing model reproduces the relationship between gene expression, E-P contact probability, and contour length. $\lambda_{off,1} = 0.11\,\mathrm{min}^{-1}$, $\lambda_{off,2} = 0.14\,\mathrm{min}^{-1}$, step interval=0.05 min, $\lambda_{on} = 0.15\,\mathrm{min}^{-1}$. $D_{EP}^{contact} = 0.7 D_{EP}^{commun}$. (a) Bursting time proportion from simulation, comparable to LacZ expression in [3], decreases as L_{EP} increases, regardless of L_{bead}. $D_{EP}^{commun} = 0.06\ \mu m$, $d_{bead} = 13$ nm. (b) Bursting time proportion from 2D (spherical surface with a radius of $10^4 \times d_{bead}$) or 3D dynamic kissing model, similar to mRNA number per cell in [4], increases with contact probability. $D_{EP}^{commun} = 0.35$ (2D) or 0.2 μm (3D). $L_{bead} = 50$ nm, $d_{bead} = 6$ nm.

Zuin et al. [4] varied E-P genomic distances by reinserting the piggyBac enhancer cassette. In our simulation, E-P contact probability was the fraction of time the E-P distance stayed below a set threshold ($D_{EP}^{contact}$). Results show that when $D_{EP}^{contact}$=D_{EP}^{commun}, gene expression scales linearly with E-P contact probability. However, E-P communication may occur beyond measurable physical contact, suggesting $D_{EP}^{commun} > D_{EP}^{contact}$. The simulation matched the observed sigmoidal relationship between gene expression and contact probability [4] only when $D_{EP}^{contact} = 0.7 D_{EP}^{commun}$. This result remained consistent across model variations [Fig. 4 (b)]. It suggests gene expression level plateaus because communication probability saturates faster than contact probability.

[1] H. Chen, M. Levo, L. Barinov, M. Fujioka, J. B. Jaynes, and T. Gregor, Dynamic interplay between enhancer–promoter topology and gene activity, Nat. Genet. **50**, 1296 (2018).
[2] J. M. Alexander, J. Guan, B. Li, L. Maliskova, M. Song, Y. Shen, B. Huang, S. Lomvardas, and O. D. Weiner, Live-cell imaging reveals enhancer-dependent sox2 transcription in the absence of enhancer proximity, elife **8**, e41769 (2019).
[3] N. Hao, K. E. Shearwin, and I. B. Dodd, Positive and negative control of enhancer-promoter interactions by other dna loops generates specificity and tunability, Cell Reports **26**, 2419 (2019).
[4] J. Zuin, G. Roth, Y. Zhan, J. Cramard, J. Redolfi, E. Piskadlo, P. Mach, M. Kryzhanovska, G. Tihanyi, H. Kohler, M. Eder, C. Leemans, B. van Steensel, P. Meister, S. Smallwood, and L. Giorgetti, Nonlinear control of transcription through enhancer-promoter interactions, Nature **604**, 571 (2022).
[5] D. B. Brückner, H. Chen, L. Barinov, B. Zoller, and T. Gregor, Stochastic motion and transcriptional dynamics of pairs of distal dna loci on a compacted chromosome, Science **380**, 1357 (2023).
[6] P. Mach, P. I. Kos, Y. Zhan, J. Cramard, S. Gaudin, J. Tünnermann, E. Marchi, J. Eglinger, J. Zuin, M. Kryzhanovska, S. Smallwood, L. Gelman, G. Roth, E. P. Nora, G. Tiana, and L. Giorgetti, Cohesin and ctcf control the dynamics of chromosome folding, Nature Genetics **54**, 1907 (2022).
[7] K. Drlica and J. Rouviere-Yaniv, Histonelike proteins of bacteria, Microbiological reviews **51**, 301 (1987).